Jet fuel chemical kinetics: shock tubes, laser diagnostics, and machine learning methods

Author: Nicolas Pinkowski

Research Advisors: David Davidson and Ronald Hanson

Affiliation: Department of Mechanical Engineering, Stanford University

Degree Status: Ph.D. Student

February/2018

Table of Contents

Abstract:

The development of kinetics mechanisms to model jet fuel combustion requires detailed information about the high-temperature pyrolysis products of these fuels. This study presents a method to measure the mole fractions of the important decompositions products, i.e. CH_4, C_2H_4, C_3H_6, i-C_4H_8, 1-C_4H_8, C_6H_6, C_7H_8, and fuel that form during thermal decomposition (pyrolysis) of conventional and alternative jet fuels. This method combines the use of shock tubes, laser absorption spectroscopy, and a mathematical method commonly employed in machine learning (convex optimization) to determine species mole fractions during pyrolysis experiments. This approach is possible because of the development of a large spectroscopic database of absorption cross sections measured for 8 species at 8 wavelengths that has recently been compiled from over 1200 shock tube measurements. Using this spectral database in conjunction with laser absorption measurements in a shock tube at 8 wavelengths, species time-histories for the decomposition products of 4 fuels (JP8, JP5, Jet A and Gevo ATJ) were measured. This represents the first effort to measure and compare a large series of fuel decomposition products for jet fuels at combustion temperatures with model results.

1. Introduction

In an effort to reduce CO_2 emissions and increase U.S. energy independence, the United States Government and aviation industry have stated their commitment to achieving carbon-neutral growth by the year 2020 [1]. Alternative jet fuel deployment is a key component of this commitment and widespread "drop in" use of alternative fuels is required in order to achieve 2020 goals. However, safety and fuel performance must not be compromised with the adoption of alternative jet fuel in today's commercial fleets. Although there are several alternative fuels certified through the new ASTM fuel standard (D7566), the standard largely focuses on physical properties in lieu of any chemical properties associated with combustion of the fuel [2]. In fact, there is no universally accepted model for the chemistry of traditional or alternative jet fuel to base a certification process off of – although there are two models emerging with promising experimental validation [3-8]. Assuming complex mixes of traditional and alternative fuels are critical to the future of the aviation industry, there is a clear need to develop accurate kinetics models. An improved fundamental understanding of how fuel composition affects combustion kinetics will greatly contribute to informing alternative jet fuel criteria and simplifying the certification process. In a broad context, this work contributes to kinetic models which will both inform next generation safety standards and facilitate the design of more efficient combustions system for aviation.

The salient barrier that has impeded model development is the complexity of jet fuel's chemical composition. Jet fuel is a very diversified mixture and containing 1000's of different compounds [3]. Figure 1 demonstrates the generalized composition of a traditional Jet A (left) compared to a bio-derived alcohol to jet fuel (ATJ) alternative fuel from the company Gevo™ (right). While the general component classifications are shown in Figure 1, the exact composition of the jet fuel is unknown, complex, and varied. Because the exact starting composition is unknown, it is intractable to model a real fuel in complete detail. Nonetheless, two methodologies have arisen that simplify the challenge of modeling jet fuel: 1) a simplified hybrid model (HyChem) [4-6] 2) a surrogate fuel model with a detailed mechanism

[7-8]. The merits of each approach are beyond the scope of the current study, which is focused on experimental measurements of species formation.

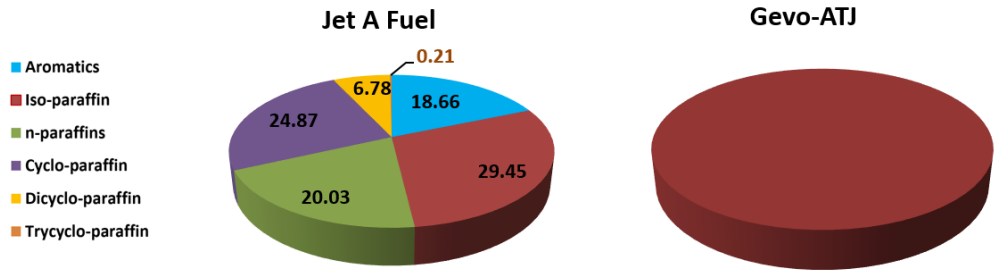

Figure 1: Jet A (left) and Gevo-ATJ fuel (right) composition - major classes of hydrocarbon compounds [3].

Time resolved species measurements during fuel pyrolysis is a method to provide validation against kinetics models and has been applied recently in the works of [9-14]. Fuel pyrolysis measurements provide a logical first step to validating a kinetic model and advancing scientific understanding of how a fuel reacts at high temperature. In such pyrolysis experiments, laser absorption spectroscopy is regarded as a well-suited technique to measure individual species within complex gas mixtures. For high temperature pyrolysis experiments, there exists non-invasive laser based methods capable of measuring methane [15], ethylene [16], propene [17-18], and isobutene [19]. There has been no combined measurement of the aforementioned species during the pyrolysis of jet fuel – although the work of Parise et al. [11] presents the combined measurement of three species. In the current study a new method is proposed to measure the formation of up to 8 small hydrocarbons expanding upon the methods of [11,15-20].

2. Experimental Design:

2.1. Shock tubes:

Experiments were preformed using a heated shock tube at Stanford University. The experimental apparatus uses a reflected shock wave to generate a region of controlled high temperature and pressure test gas. For a general representation, Figure 2.a. is used to depict the end wall of a shock tube and passage of the reflected shock. A full discussion on the shock tube facility is provided by Parise et al. [11]. Figure 2.b presents a representative shock tube experiment with a test gas of 5% 1-butene/Ar heated to 1220 K and 1.73 atm. Three zones are visible in Figure 2: 1) an initial region with low pressure and temperature, 2) a second region after the passage of the shock wave at intermediate pressure and temperature, and 3) a final region after the passage of the reflected shock wave at the highest pressure (1.73 atm) and temperature (1120 K) test conditions. Time zero is established by the passage of the reflected shock wave at the diagnostic location and is assumed to mark the moment at which fuel pyrolysis begins.

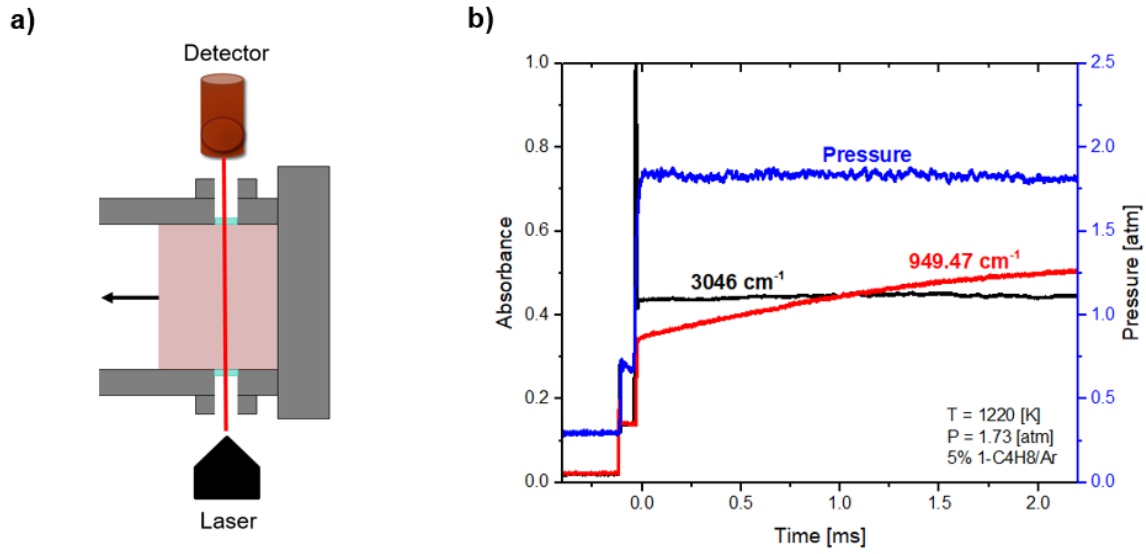

Figure 2: a) diagram of the test section of a shock tube with reflected shock shown traveling left. b) a shock tube experimental pressure, absorbance at 3046 cm^{-1} (3.283µm), and 949.47cm^{-1} (10.532 µm) are shown for the pyrolysis of 5% 1-C4H8/Ar. The reflected shock temperature and pressure are 1220 K and 1.73 respectively. Temperature was calculated using a standard FROSH simulation [21].

2.2. Laser Diagnostics:

Laser measurements are used measure the absorbance of different colors of light aligned through the test section of the shock tube. As different species interact with different wavelengths of light differently, multiple wavelengths of light can be used to measure the concentration of certain species in an experiment. Absorbance, α of species *i,* at wavelength, λ is calculated using the Beer-Lambert Relation:

$$\alpha_{i,\lambda} = -\ln\left(\frac{I_\lambda}{I_{\lambda.0}}\right) = \sigma_{i,\lambda}(T,P)nx_iL \qquad \text{Eq. 1}$$

Where I_λ is the transmitted laser intensity at wavelength λ, $I_{\lambda.0}$is the incident laser intensity at wavelength λ, $\sigma_{i,\lambda}(T,P)$ is the absorption cross section [m^2mol^{-1}] of species i at wavelength λ, which is in general a function of temperature and pressure, n is the number density, x_i is the mole fraction of species i, and L is the laser path length through the absorbing medium.

The total absorbance of a gas mixture of multiple species at wavelength λ is given by:

$$\alpha_\lambda = \sum_{i=1}^{N} \sigma_{i,\lambda}(T,P)Px_iL \qquad \text{Eq. 2}$$

where N is the total number of species in the gas mixture. In principle, the unknown mole fractions of N species can be determined by measuring the absorbance of a gas mixture at least N different wavelengths of light – assuming all absorption cross sections are known and that other species present do not absorb at the wavelengths chosen.

A total of 8 wavelengths of light (produced by 5 lasers) were used in this study to measure the mole fractions of 8 species. The current study used two Interband Cascade Lasers (ICL)'s provided by Nanoplus GMBH™ to probe three wavelengths (3148.81 cm^{-1}, 3148.66cm^{-1}, and 3046 cm^{-1}). Additionally, the current study used a HeNe gas laser operating at 3.39 μm (2948.11cm^{-1}), along with a common-mode rejection system that uses two detectors to reduce noise from high frequency variations of laser output. A CO_2 gas laser provided by Access Laser™ was operated at 10.532 μm (949.47cm^{-1}) and

10.675 μm (936.41cm^{-1}). The fifth laser used was a Daylight Solutions^{TM} External Cavity Quantum Cascade Laser (ECQCL) laser operated at 10.96μm (912.57cm^{-1}) and 11.345 μm (881.42cm^{-1}). The lasers were detected using two types of detectors: cryogenically cooled detectors from InSb InfraRed Associates, and thermoelectrically cooled MgCdTe detectors from Vigo Systems.

Wavelength selection:

Small hydrocarbons present in the pyrolysis products of jet fuel have dissimilar mid-IR absorption spectrums. This dissimilarity presents an opportunity to discern individual species amongst a complex mixtures of species. By probing the absorption spectrum of an unknown test gas at discrete wavelengths and comparing it to the measured absorbance of known species, the composition of the gas can be determined. Optimal wavelengths have a large absorption coefficient of one species and low absorption coefficient for all other species. Figure 3 presents the mid-IR spectrum (focused near 3 μm and 10.5 μm) for the dominate hydrocarbons expected in the pyrolysis products of jet fuel. The 8 dashed lines in Figure 3 indicate the chosen wavelengths used for the current study. The wavelengths were primarily selected from previously established diagnostics, however, two new diagnostics were first applied here. The wavelengths with high sensitivity to methane at 3175.80 μm and ethylene at 10.532μm were developed in the work of [15] and [16, 17] respectively. The diagnostic with high sensitivity to propene at 10.958μm was developed in the combined work of [18, 19] and isobutene at 11.345μm in the work of [20]. An aromatics diagnostic at 3.283μm with high sensitivity benzene and toluene is first used in this work as well as a method to estimate 1-butene mole fractions from residual absorbance at 3.39 μm. The wavelength 3175.85 μm is used to measure the background absorbance in the 3 μm region and contributes to measuring aromatics and 1-butene.

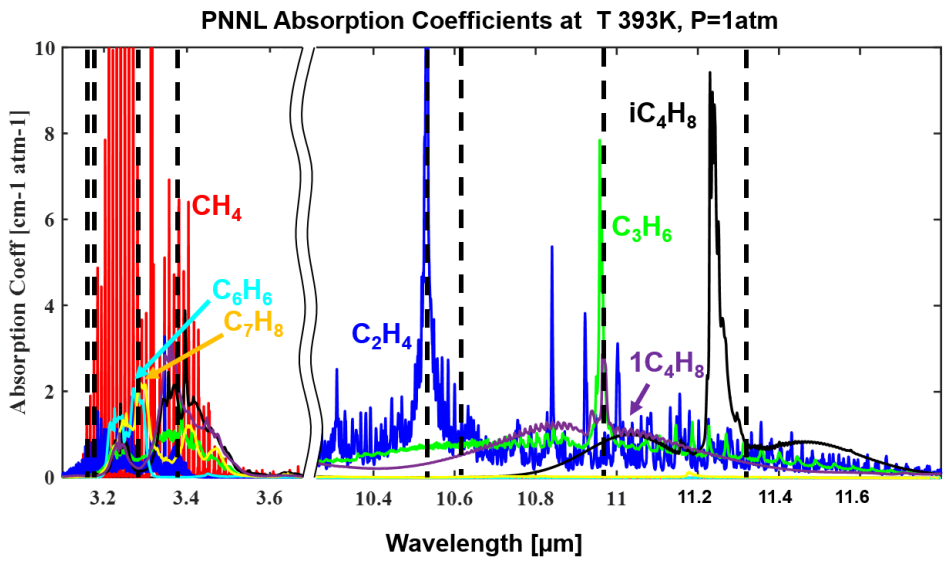

Figure 2: Example spectrum of common products of jet fuel decomposition from PNNL Spectral database [23]. The 3 µm region provides salient absorption features of a C-H stretch dominated by alkane and aromatic compounds, where the 10-12 µm region provides salient absorption features of small, non-saturated, hydrocarbons and vibrations associated with carbon-carbon double bonds dominated by alkene compounds.

3. Measurements

3.1. Cross-sections and cross section database

In order to solve for mole fractions as a convex optimization problem, the absorption cross-section must be known for all species at each wavelength as a function of temperature. At low temperatures, absorption cross sections have been measured by Fourier transform infrared spectroscopy (FTIR) and are available. The PNNL spectral database provides an example of available low temperature cross-sections and Figure 3 presents the PNNL cross sections at low temperature for dominate pyrolysis products. Inopportunely, at high temperature no spectroscopic database yet exists. Accordingly, as part of the current study, all cross sections required for each species and wavelength were measured and compiled. A cross section measurement can be extracted from an experiment like that shown in Figure 2 - where the absorbance at the beginning of the test time for each color can be attributed to only 1-butene. Taking the

absorption cross section of argon at all wavelengths as zero, $\sigma_{i,\lambda}$ may be calculated using Equation 2. Figure 4.a and 4.b provide example absorption cross section results for a) ethylene at several wavelengths and b) propene at several wavelengths respectively. An experiment, like that of Figure 2, would provide two data points for a similar plot as Figure 4 for isobutene. The cross sections measurements collected at 8 wavelengths and 11 species (CH_4, C_2H_4, C_3H_6, i-C_4H_8, 1-C_4H_8, C_6H_6, C_7H_8, Jet A, Gevo-ATJ, JP8, JP5) represent the combination of approximately 1200 shock tubes experiments. In total, 88 temperature dependent cross-section expressions were tabulated and used in the computation of mole fraction.

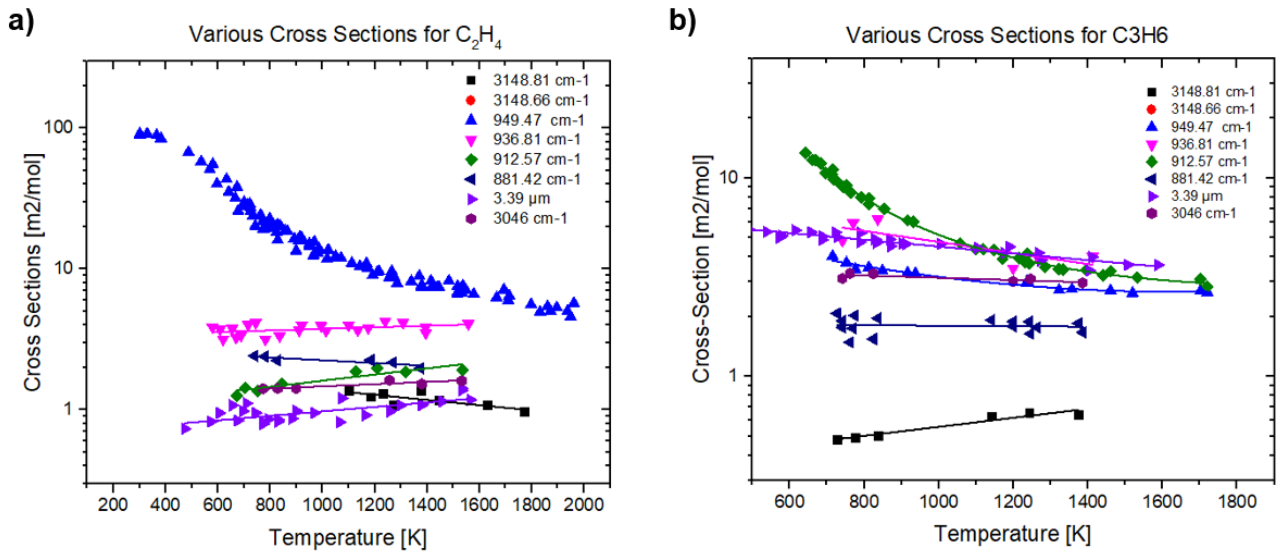

Figure 3: Example absorption cross sections for a) C_2H_4, and b) C_3H_6 at various wavelengths. The temperature on the abscissa corresponds the FROSH calculated temperature of a reflected shock tube experiment. Cross-section experiments use with argon as a diluent. For high temperatures, the absorbance immediately after time zero was used for the calculation of the cross-section in Equation 2. All measurements taken between 1-2 atm.

3.2. **Jet fuel absorbance**

Following the measurement of the absorption cross-sections, this study measures the time-variant absorbance during the high temperature pyrolysis (from T=1100-1350K) for Jet A, and Gevo ATJ at each of the 8 wavelengths and at pressure between 1.5-2 atm. This study recorded and compiled a database of

the time resolved absorbance data for over 300 jet fuel shock tube measurements, 14 of which are shown in Figure 5 for 3.39 µm and 3.28 µm for Gevo ATJ. Each absorbance trace was fit to a double exponential curve and the parameters were stored along with the experimental conditions. The parameters for each condition were then used to approximate the absorbance of a given wavelength, for a certain fuel type, for a given temperature and pressure. The simulated absorbances and their fits are shown as dashed lines for each temperature on Figure 5.

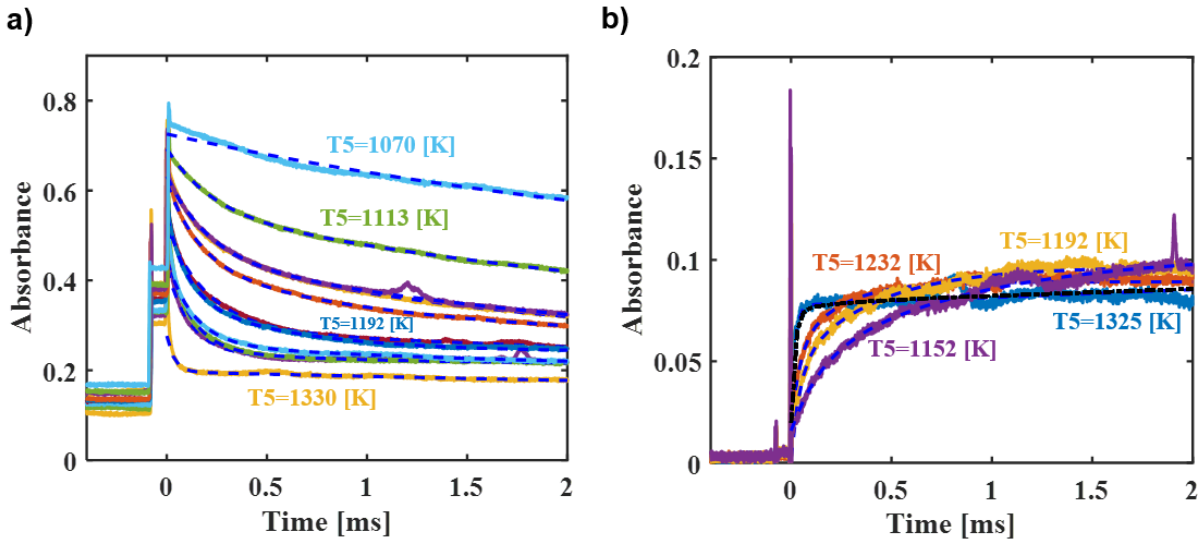

Figure 4: Example absorbance measurements for Gevo-ATJ fuel and their fits for a range of temperatures. a) for 3.39 µm (2948.11 cm^{-1}) and b) for 10.958 µm (912.57cm^{-1}). Pressures for each experiment ranged from 1.5-2 atm, and initial fuel loading was 0.4% Gevo-ATJ/Argon. The shock tube and mixing manifold were at elevated the experimental procedure was the same as the methods developed by Parise et al. [11].

4. Data reduction

4.1. Overview | Approximation of mole-fractions from absorbance

This study proposes a method to estimate species mole fractions using measured cross-sections and absorbance traces from the fuel pyrolysis experiments. Using the database of absorbance trace fits across a variety of experimental conditions it is possible to interpolate between experimental conditions to simulate what the experimental absorbance would be at any of the 8 studied wavelengths at any

temperature and pressure between 1100-1350K and 1.5-2.0 atm. Thus, from 0-2 ms (the standard test time) a simulated absorbance profile is generated for the 8 wavelengths. The absorbance "simulations" are interpolations based directly on measured experimental data. Using Equation 2 this study generates a system of 8 wavelengths and 8 unknown mole-fractions at each time step from 0-2 ms. A system of equations can be solved at each point in time to determine mole fractions for all 8 species. However, as given in Equation 2 the absorbance cross section requires temperature and pressure. The shock tube experiments are conducted at constant pressure which is directly measured and known. However, the estimation of temperature warrants further discussion.

4.2. *Temperature dependence of the absorption cross-section:*

The absorption cross sections are a function of temperature and therefore an estimate of the temperature change during a pyrolysis experiment is required. The initial temperature of the test gas after time zero is determined using a standard FROSH reflected shock calculation developed for shock tube experimentation [21]. To estimate the temperature decrease during the endothermic fuel pyrolysis process, this study relies on a modeled temperature profile using a HyChem simulation ran at constant pressure [3-6]. While this is a standard estimation method, future studies may include a spectroscopic measurement of temperature to obviate the need for interplay between model development and measurement.

4.3. Convex Speciation:

With the temperature, cross-sections, and absorbance traces, an estimation of the mole fraction can be made. The absorption at each wavelength from Equation 2 is reformatted here:

$$\sigma_{CH4,\lambda_1} x_{CH4} + \sigma_{C2H4,\lambda_1} x_{C2H4} + \cdots \sigma_{i,\lambda_1} x_i = \frac{\alpha_{\lambda_1}}{nL} \qquad \text{Eq. 2}$$

(at wavelength c1/c2)

$$\sigma_{CH4,\lambda_2} x_{CH4} + \sigma_{C2H4,\lambda_2} x_{C2H4} + \cdots \sigma_{i,\lambda_2} x_i = \frac{\alpha_{\lambda_2}}{nL}$$

… (for 8 wavelengths)

Reformatting Eq. 2 into a matrix format for absorption cross-sections and mole fractions:

$$\mathrm{K} = \begin{bmatrix} \sigma_{1,1} & \cdots & \sigma_{1,N} \\ \vdots & \ddots & \vdots \\ \sigma_{m,1} & \cdots & \sigma_{m,N} \end{bmatrix} \quad , \; \vec{x} = \left[x_{CH_4},\; x_{C_2H_4},\; x_{C_3H_6},\; x_{iC_4H_8},\; x_{1C_4H_8},\; x_{C_6H_6},\; x_{C_7H_8},\; x_{Gevo\,ATJ} \right]^T$$

Where the rows are the m different wavelengths of light and the columns are the N different species. We now apply the Beer-Lambert Relation in a matrix form:

$$\mathrm{K}\vec{x} = \vec{b} \qquad \text{Eq. 3}$$

Such that $\vec{b} = \frac{\alpha_c}{nL}$ for each of the eight wavelengths and where $\mathrm{K} \in \mathbb{R}^{\mathrm{mxN}}$ is the absorption cross-section matrix. In order to solve Equation 3 for the mole fraction vector this study frames the problem as a convex optimization problem. The convex problem solved at each time step using the following objective function:

$$Minimize\text{: } \left\| \mathrm{K}\vec{x} - \left(\vec{b} - S\right) \right\|_2^2 \qquad \text{Eq. 4}$$

Under the given constraints:

1. The total carbon in the system must be less than or equal to known carbon at time zero
2. The calculated mole fraction of each species must be greater than or equal to zero
3. The calculated amount of jet fuel must be monotonically decreasing
4. There can be some amount of interfering absorbance, S, at 3.39 μm from unaccounted C-H stretch vibrations
    a. $0 \leq S_{3.39} \leq \frac{1}{2} b_{3.39}$

Equation 4 under the given constraints can be solved readily using a standard convex optimization solving platform. The current study used MATLAB CVX software developed by CVX Research Inc. [24-25]. A qualitative description of the variable $S_{3.39}$ is that the system will find the minimum of the objective function for all potential interfering absorbance at 3.39μm. Accordingly, the lowest possible objective function for the given mole fractions and inference variable is the optimal solution. Additional

interference variables (similar to $S_{3.39}$) may be added at other wavelengths likely to have interfering species (like 11.345μm or 3.28μm), however, the solution has not been found to change significantly. The mole fractions of CH_4, C_2H_4, C_3H_6, i-C_4H_8, 1-C_4H_8, C_6H_6, C_7H_8, and fuel are extracted for Jet A and Gevo ATJ. Because the mole fractions measured in this study account for over 76% of all carbon for Jet A, and 97% of all carbon for Gevo-ATJ, any potential interfering species are assumed to exist in small concentrations and contribute exiguously to the interference at each wavelength. Therefore, without conclusive evidence to support a more complex solution method, the current study only uses one interference variable.

4.4. Error calculation

Because the current convex problem is classified as a constrained least squares problem, the estimated error for this relied upon the error estimation for least squares fitting methods [26]. Future studies can rigorously include the error in the cross-sections and the absorption measurements by framing the problem as a stochastic robust approximation problem as detailed in the work of Boyd [27]. For example, in such a problem the absorption cross-section matrix that would be used is: $\overline{K} = K + error$ and the objective function would include the expectation: $E\left[\left\|\mathrm{K}\vec{x} - (\vec{b} - S)\right\|_2^2\right]$.

5. Results

Using the aforementioned solution method, the mole fractions of CH_4, C_2H_4, C_3H_6, i-C_4H_8, 1-C_4H_8, C_6H_6, C_7H_8, and fuel can be estimated during the pyrolysis of a traditional fuel Jet A and Gevo-ATJ. Following, this section compares the measured gas composition for Jet A and Gevo-ATJ at 2 ms after pyrolysis of 0.4% fuel/Ar for an initial shock heated temperature of 1310 K, and a pressure of 1.8 atm. Figure 6 presents the 2 ms yields for each 8 species, and for comparison, also includes the computed yields of the HyChem model at 2 ms. The yield is defined as the measured mole fraction at 2 ms divided by the initial mole fraction of fuel (0.4%fuel/Ar).

With few exceptions, results show that 2 ms yields are in agreement with the model. The largest deviation between model and measured occurs in ethylene for Jet A and propene for Gevo-ATJ. For aromatics, the bio-derived jet fuel is observed to form significantly less aromatics (benzene and toluene) during the 2 ms test time than Jet A. Aromatic compounds are present in the initial composition of Jet A and absent in Gevo-ATJ, thus, the aromatics yields at 2 ms can be attributed to the initial composition. Concerning the rate of fuel decomposition, the current study measures nearly complete decomposition of the fuel by 2 ms. For butenes, 1-butene and isobutene yields are measured to be higher for Jet A than predicted, yet within the experimental error provided. The discrepancy between the modeled and measured mole fractions for propene, 1-butene, isobutene, and aromatics is appreciable though accounted for within error bounds of the current study. In both Jet A, and Gevo-ATJ over 76% and 97% of the carbon in the system is accounted for at 2 ms respectively.

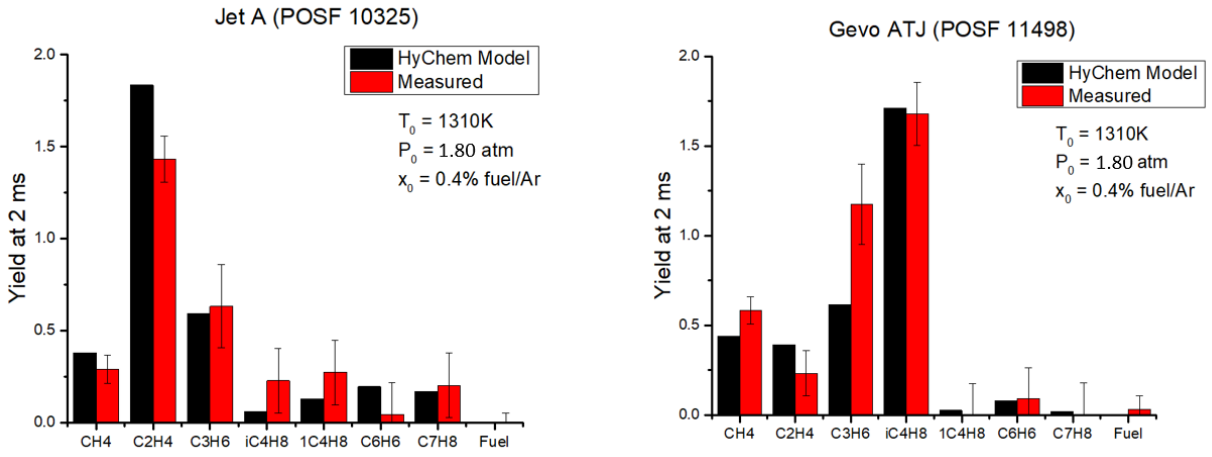

Figure 5: Yields (measured mole fractions divided by initial fuel mole fraction) at 1310K, 1.8 atm, and 0.4% fuel loading in Argon. (left) Jet A, (right) Gevo-ATJ

6. Conclusions:

The FAA has set forth to displace 1 billion gallons of jet fuel by the year 2020 [1]. Nonetheless, it is important to recognize that alternative fuels do not have the same testing history as traditional fuels. Accordingly, it is important to develop a firm understanding of the fundamental influence that fuel composition will have on the combustion process. The first step to affirming a fundamental understanding of jet fuel combustion is to measure and understand the pyrolysis process at high temperatures. For this reason, the current study presents a new method to measure the fundamental species evolution during pyrolysis experiments.

Using a new approach that relies upon the results of over 1500 shock tube measurements this study used 8 wavelengths to estimate the mole fractions of CH_4, C_2H_4, C_3H_6, i-C_4H_8, 1-C_4H_8, C_6H_6, C_7H_8, and fuel. The calculation of the mole fractions is carried out as a convex optimization problem that uses a compilation of absorption cross-sections, fuel pyrolysis absorbance traces, and simulated temperature profiles. Convex optimization is a key component of many machine learning problems today and is a valuable tool applied to jet fuel kinetics studies.

From the measurements of the species yields, key differences are observed in the pyrolysis of a traditional and alternative jet fuel. First, the dominate species formed during pyrolysis are different for each fuel: ethylene for Jet A fuel and isobutene for Gevo alternative fuel. Although GEVO-ATJ breaks down at a faster rate, the products it forms are larger and will transport at a slower rate. Secondly, significantly less aromatics are formed during the decomposition of the alternative fuel than the traditional fuel. As detailed in [28], aromatics yields are an important fuel characteristic due to the potential positive and negative impacts to the engine. For example, some fraction of aromatics is needed to maintain appropriate lubricity of seals within the engine, however, aromatics increase sooting propensity which leads to harmful emissions. Thus, it is important to recognize the decreased yield of aromatics that may form when an alternative fuel is mixed in with a traditional fuel.

Lastly, there are several methods that can decrease experimental error and increase the total percentage of carbon accounted for. Future studies may include adding additional wavelengths in both the 3-4 μm region and 10-12μm region. The author suggests 3.41 μm as an appropriate wavelength which could use the cross section measurements from Wang et al. [22]. The author also encourages the development of a new diagnostic with high sensitivity to ethane in the 3-4μm region to greatly increase the carbon recovery for Jet A.

In summary, improved measurements of fuel pyrolysis can accelerate model development and provide an experimental validation tool for any model. As alternative jet fuels grow in prevalence, speciation measurements will be a key component to measure how a varied fuel composition impacts combustion.

Acknowledgements: This work was funded by the US Federal Aviation Administration (FAA) Office of Environment and Energy as a part of ASCENT Project 25 under FAA Award Number: 13-C-AJFE-SU-016. Any opinions, findings, and conclusions or recommendations expressed in this material are those of the authors and do not necessarily reflect the views of the FAA or other ASCENT sponsors. The author would also like to provide great thanks to the Department of Defense and NDSEG Fellowship program.

References:

[1] Federal Aviation Administration, 2015. Aviation Greenhouse Gas Emissions Reduction Plan.
[2] ASTM International. D7566-17a. Standard Specification for Aviation Turbine fuel containing Synthesized Hydrocarbons
[3] Wang H., Xu R., Hanson R., Davidson D., Egolfopoulos F. Liquid, Real-fuel Combustion Kinetics – I. Evidence Supporting a Physics-Based Approach. Submitted to Combustion and Flame July, 2017.
[4] Xu R., Chen D., Wang K., Shao J. et al. HyChem Model: application to Petroleum-Derived Jet Fuels
[5] Wang K., Xu r., Shao J., Davidson et. al. Evaluation of a Hybrid Chemistry Approach for Combustion of Belnded Petroleum and Bio-derived Jet Fuels. 10th U. S. National Combustion Meeting paper
[6] Xu R., Chen D., Wang K., Wang H., A comparative study of combustion chemistry of conventional and alternative jet fuels with hybrid chemistry approach. 10th U. S. National Combustion Meeting paper 2017. DOI: 10.2514/6.2017-0607
[7] Malewicki T., Gudiyella S., Brezinsky K. Experimental and modeling study on the oxidation of Jet A and the n-dodecane/iso-octane/n-propylbenzene/1,3,5-trimethylbenzEne surrogate fuel. Combustion and Flame 160 (2013) 17-30
[8] Dooley S., Won S., Chaos M., Heyne J., Ju Y., Dryer F., Kumar K., Sung C., Wang H, Oehlschlaeger M., Santoro R., Litzinger T. A Jet fuel surrogate formulated by real fuel properties. Combustion and Flame 157 (2010). 2333-2339
[9] J.K. Shao, D.F. Davidson and R.K. Hanson, "Shock Tube Study of Jet Fuel Pyrolysis and Ignition at Elevated Pressure," submitted to 10th U.S. National Combustion Meeting.
[10] Y. Zhu, S. Wang, D.F. Davidson and R.K. Hanson, "Shock Tube Measurements of Species Timehistories during Jet Fuel Pyrolysis and Oxidation," 25th ICDERS Conf., Leeds, UK, Aug. 2-7, 2015.
[11] T. Parise, D.F. Davidson and R.K. Hanson, "Shock Tube/Laser Absorption Measurements of the Pyrolysis of a Bimodal Test Fuel," 36th Symp. (Int.) on Combustion, Seoul, Korea, 2016 DOI 10.1016/j.proci.2016.07.081
[12] D.F. Davidson, A. Tulgestke, Y. Zhu and R.K. Hanson, "Species Time-history Measurements during Jet Fuel Pyrolysis and Oxidation," ISSW 30/Tel Aviv, 7/2015 DOI 10.1007/978-3-319-46213-4_51
[13] Y. Zhu, R.K. Hanson and D.F. Davidson, "Shock Tube/ Laser Absorption Measurements of Jet Fuel Pyrolysis and Oxidation," 53rd AIAA Aerospace Sciences Meeting, Kissimmee, FL 1/2015 DOI 10.2514/6.2015-1158
[14] S. Li, Y. Zhu, D.F. Davidson and R.K. Hanson, "Pyrolysis Study of Conventional and Alternative Fuels behind Reflected Shock Waves," Fuel 132 170-177 (2014) DOI 10.1016/j.fuel.2014.04.077
[15] R. Sur, S. Wang, K. Sun, D.F. Davidson, J.B. Jeffries and R.K. Hanson, "High Sensitivity Interference free Diagnostic for Measurement of Methane in Shock Tubes," JQSRT 156 80-87 (2015) DOI 10.1016/j.jqsrt.2015.01.023
[16] W. Ren, D.F. Davidson and R.K. Hanson, "IR Laser Absorption Diagnostic for C2H4 in Shock Tube Kinetics Studies," IJCK 44 (2012) 423-432 DOI 10.1002/kin.20599

[17] M.E. MacDonald, W. Ren, D.F. Davidson, R.K. Hanson, W. Pitz, M. Mehl and C.K. Westbrook, "Fuel and Ethylene Measurements during n-Dodecane, Methylcyclohexane and iso-Cetane Pyrolysis in Shock Tubes," Fuel 103 1060-1068 (2013) DOI 10.1016/j.fuel.2012.09.068

[18] Parise T., Davidson D., Hanson R. Development of a Two-Wavelength IR laser Absorption Diagnostic for Propene and Ethylene. Submission to Measurement, Science and Technology Journal 2/12/2018

[19] Chrystie R, Nasir EF, Farooq, A. Applied Physics B 2015, 120: 317-327.

[20] R.M. Spearrin, S. Li, D.F. Davidson, J.B. Jeffries and R.K. Hanson, "High-temperature Iso-butene Diagnostic for Shock Tube Kinetics using a Pulsed Quantum Cascade Laser near 11.3 μm," Proc. Comb. Inst. 35 3645-3651 (2015) DOI 10.1016/j.proci.2014.04.002

[21] Matthew F. Campbell, Daniel R. Haylett, David F. Davidson, and Ronald K. Hanson. AEROFROSH: A Shock condition calculator for multi-component-fuel aerosol-laden flows. Shock Waves. (2016). Vol 26, pp429-447

[22] S. Wang, T. Parise, S.E. Johnson, D.F. Davidson and R.K. Hanson, "A New Diagnostic for Hydrocarbon Fuels using 3.41-micron Diode Laser Absorption," Comb. and Flame 186 129-139 DOI 10.1016/j.combustflame.2017.07.026

[23] Sharpe S., Johnson T., Sams R., Chu P., Rhoderick G., Johnson P. Gas-Phase Databases for Quantitative Infrared Spectroscopy. (2004). Society for Applied Spectrscopy. V 58. No. 12, 2004 pg. 1452-61

[24] CVX Research, Inc. CVX: Matlab software for disciplined convex programming, version 2.0. http://cvxr.com/cvx, April 2011.

[25] M. Grant and S. Boyd. Graph implementations for nonsmooth convex programs, Recent Advances in Learning and Control (a tribute to M. Vidyasagar), V. Blondel, S. Boyd, and H. Kimura, editors, pages 95-110, Lecture Notes in Control and Information Sciences, Springer, 2008. http://stanford.edu/~boyd/graph_dcp.html

[26] Richter P., Estimating Error in Least-Squares Fitting. Nasa TDA progress Report 42-122. August 15, 1995

[27] Boyd S., Vandenberghe L. Convex Optimization Cambridge University Press. (2004).

[28] M. Colket , T. Edwards , S. Williams , et al. , in: 46th AIAA Aerospace Sciences Meeting and Exhibit, 2008 AIAA 2008-972 .